High spectral efficiency superchannel transmission using a soliton microcomb

N.B. When citing this work, cite the original published paper.

(article starts on next page)

High Spectral Efficiency Superchannel Transmission using a Soliton Microcomb

Mikael Mazur[1]* , Myoung-Gyun Suh[2], Attila Fülöp[1,3], Jochen Schröder[1], Victor Torres-Company[1], Magnus Karlsson[1], Kerry J. Vahala[2] and Peter A. Andrekson[1]

[1]*Photonics Laboratory, Chalmers University of Technology, SE-41296, Gothenburg, Sweden*
[2]*T. J. Watson Laboratory of Applied Physics, California Institute of Technology, Pasadena, CA 91125, USA*
[3]*Now at OptiGOT AB, Hugo Grauers gata 3B, SE-41133 Gothenburg, Sweden.*
*E-mail: mikael.mazur@chalmers.se

Keywords: Optical fiber communication, frequency combs, Soliton microcomb, integration

Abstract

We demonstrate transmission of a 52 channel superchannel using an optimized 22.1 GHz-spaced soliton microcomb. Enabling a record spectral efficiency of >10 bits/s/Hz after 80 km and 6.1 bits/s/Hz after 3000 km using a microcomb. Our results demonstrate that chip-scale combs can achieve performance directly comparable to bulk-optic frequency combs.

1 Introduction

The drive for increasing both the throughput and the efficiency of optical communication systems has increased the focus on spectral efficiency (SE) [1]. Modern transponders use high-order polarization-multiplexed M-ary quadrature amplitude modulation (PM-MQAM) such as PM-64QAM to encode >10 bits per transmitted symbol. The system throughput is further increased using wavelength division multiplexing (WDM), exploiting the broad gain bandwidth of erbium-doped fiber amplifiers (EDFAs).

To fill the about 10 THz C+L-band bandwidth, >300 transceivers are needed assuming symbol rates of about 30 Gbaud. For such systems, the SE is limited by the available signal to noise ratio (SNR) and required guard-bands between channels. The guard-bands are needed to avoid catastrophic channel overlaps originating from drifts in the laser frequencies. Using standard external cavity lasers (ECLs), a few GHz guard-band is usually needed [2]. The SNR limitation accounts for noise from the transceiver, such as limited effective number of bits (ENOBs) and timing jitter. In addition, the SNR is limited by added noise from EDFAs and non-linear distortions from the transmission link.

Optical frequency combs have been suggested as a replacement for laser arrays as WDM carriers [3, 4]. A frequency comb is a coherent multi-wavelength light source which is fully characterized its center frequency f_0 and line spacing Δf. Another very beneficial property of using a comb is that it avoids the problem of drifts from free-running lasers. This was exploited in [5], demonstrating a SE of 17.3 bits/s/Hz for a 10 channel superchannel with 3 Gbaud channels and an electro-optic frequency comb. Densely packed superchannels also avoid large guard-band allocation in optically routed networks which drastically improves network SE [1].

To make superchannels even more attractive, integration is needed [6]. Integrated combs offer small foot-print with large potential for power savings compared to bulk-optic combs or laser arrays [6, 7]. The development of single soliton Kerr frequency combs have recently enabled multiple applications such as frequency synthesis [8] and improved atomic clocks [9]. For data transmission, multiple Kerr-comb states have been investigated [10–13]. Soliton microcombs are also suitable for use in optical transmission systems as the flat envelope minimize variations in optical SNR (OSNR) for individual lines. In [6], 50 Tbit/s throughput over a 75 km link was demonstrated. The large Δf of 100 GHz limited the SE to 2.8 bits/s/Hz using a single comb. For microcombs, balancing the comb width (to ensure sufficient OSNR) while targeting a Δf around 10-30 GHz to balance transceiver count and performance of electronics has proven very challenging. Following this, to date, the SE demonstrated using integrated sources has been far away from the >10 bits/s/Hz SE achieved using 20-30 GBaud channels and bulk-optic combs [14].

In this work we demonstrate transmission of a 52×21.5 Gbaud PM-16/64/256QAM comb-based superchannel using a 22.1 GHz soliton micro-comb. The comb is optimized to focus the line power to the about 10 nm bandwidth of the superchannel. With $\Delta f = 22.1$ GHz, the high performance DAC/ADC can modulate the full channel width. The stability of the comb permits dramatic reduction of the inter-channel guard-bands to sub-GHz level, allowing us to maximize the system's total spectral efficiency. We demonstrate a record high spectral efficiency of 10.4 bits/s/Hz after a single 82 km standard single-mode fiber (SSMF) span using a microcomb. In addition, we perform the first long-haul transmission experiment using an integrated comb source together with dense WDM and advanced modulation formats, achieving a spectral efficiency of 6 bits/s/Hz after >3000 km using a recirculating loop with EDFA-only amplification. Demonstrating performance directly comparable to bulk-optic frequency combs, our results show that microcombs can enable high performance integrated superchannel transceivers.
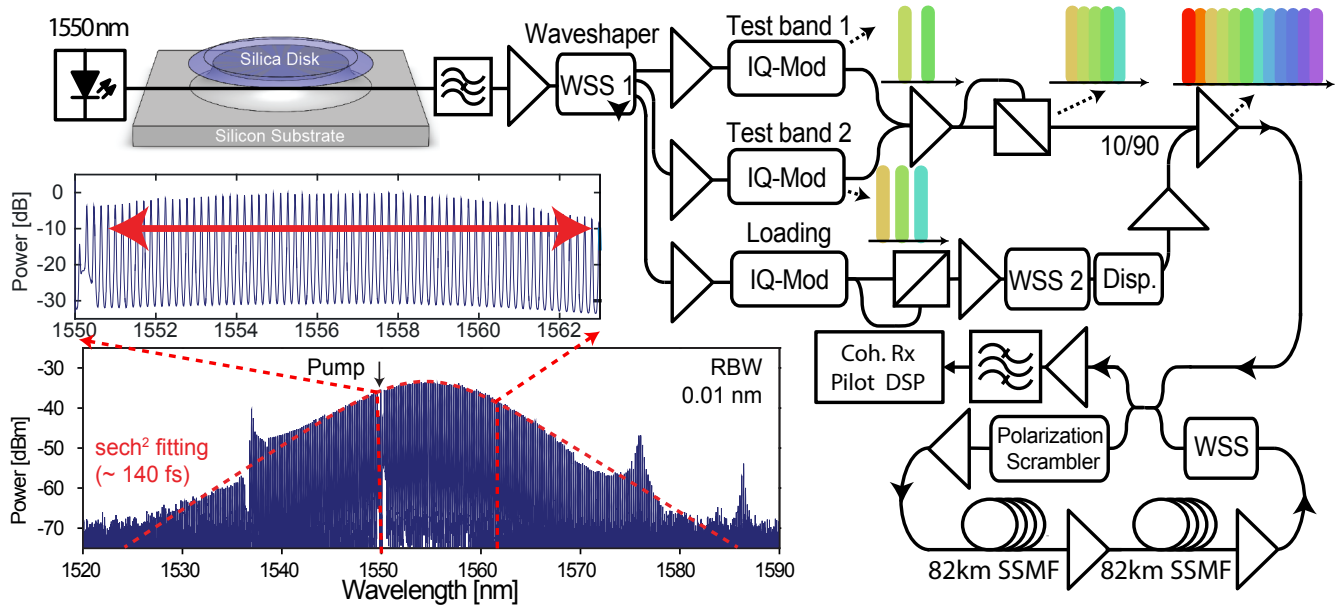
Fig. 2 Experimental setup for comb-based superchannel transmission. The silica disk resonator generated a 22.1 GHz spaced frequency comb which was modulated using a test-loading-band approach and transmitted through the recirculating loop. Fitting a sech^2 to the output comb envelope results in an estimated pulse width of about 140 fs. The horizontal red arrow in the zoom-in spectrum marks the 52 lines (8 dB flatness) used to modulate the superchannel.

2 Microcomb

We used a high-Q whispering-gallery-mode silica resonator [15] to generate the soliton frequency comb with a 22.1 GHz repetition rate. To facilitate system evaluation and thermal stability, the device was packaged together with a thermoelectric cooling element in a compact module (30 mm x 94 mm x 15 mm) as shown in Fig. 1. We used about 150 mW pumping power to initialize the comb (the initialization process is described in [16]). The resulting comb spectra is shown in Fig. 2, with the red arrow showing the lines used to form the superchannel. The comb was pumped at 1549.9 nm and to facilitate high SE data transmission by not having to sacrifice any lines surrounding the pump, we used the Raman self-frequency shift [17] to displace the spectral center to around 1555 nm. The comb flatness was 8 dB over the 10 nm bandwidth used to form the superchannel. We measured the Δf drift to be below 100 kHz over several hours, concluding that variations in line spacing will not affect the performance of the transmission system. To facilitate long-term operation we used a temperature feedback to ensure stable operation over >100 hours.
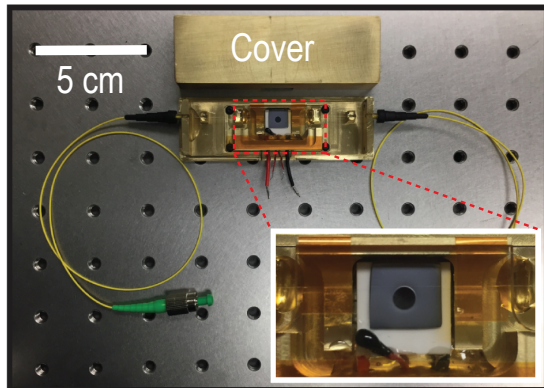

Fig. 1. Packaged micro-comb device.

3 Experimental setup

The experimental transmission setup is shown in Fig. 2. After generating the comb, a 0.3 nm notch filter was used to remove the pump before amplification with an EDFA (about 5.5 dB noise figure). A WSS was then used to separate the lines between a test band (TB) and a loading band (LB) to avoid OSNR degradation in the transmitter originating from not having one modulator per channel. The TB consisted of 5 lines which were divided into even and odd lines using the WSS. These lines were modulated using two independent IQ-modulators driven by two 60 GS/s DACs each. The modulator outputs were then combined and a PM signal was emulated using the split-delay-combine method with >250 symbol delay. The remaining 47 lines were modulated using a single IQ-modulator to form the LB. Following PM emulation, the LB was amplified and another WSS was used to carve out a notch on the position of the TB. The loading channels were then decorrelated using about 15 km of large effective area fiber before being combined with the TB to form the final superchannel.

For the single span evaluation, the superchannel was transmitted through an 82 km span of SSMF with about 16 dB loss. For the long-haul experiment, we used a recirculating loop consisting of two equivalent spans of SSMF. In addition, a band-pass filter, a WSS and a polarisation scrambler was used inside the loop. At the receiver, a 0.3 nm filter was used to select the channel under test before coherent detection and digitization using a 50 GS/s real-time oscilloscope. The waveforms were processed offline using a pilot-based DSP (available online [18]) with 0.4% pilot overhead (OH) for carrier phase estimation (CPE) and 1% and 2% OH for synchronisation and equalisation for single span and long-haul
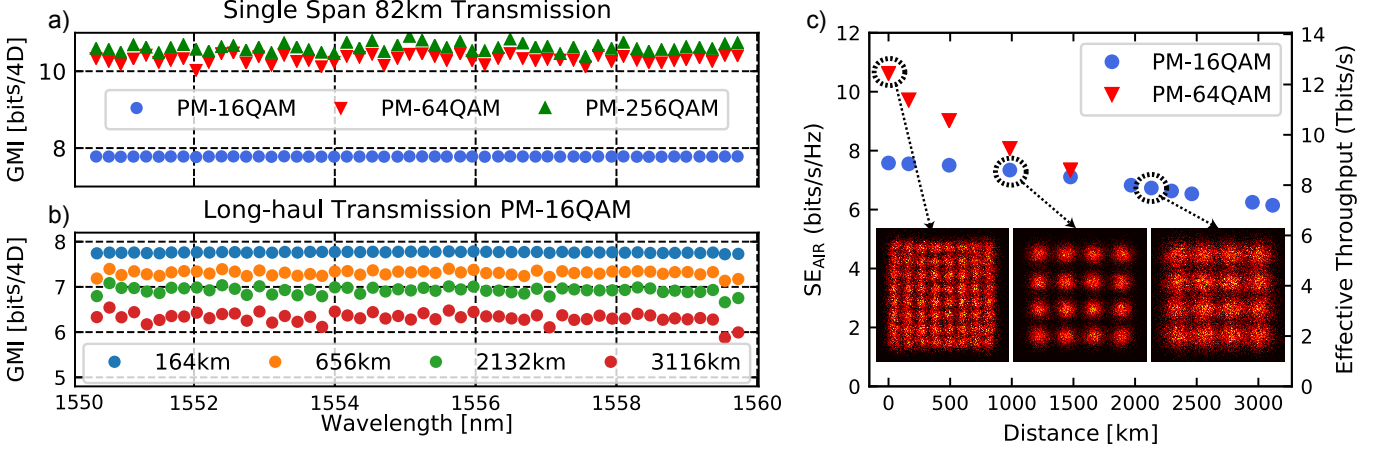
2

Fig. 4 a) Measured GMI after single span transmission for PM-16/64/256QAM. b) Measured GMI after 164, 656, 2132 and 3116 km transmission using PM-16QAM. c) Combined superchannel spectral efficiency and throughput as a function of distance. Inset shows selected constellation diagrams for center wavelength (1555.08 nm, X-pol).

transmission, respectively. The OHs were optimized to maximize the SE, similar to [14]. For the long-haul experiment, we used a hybrid pilot and blind phase search algorithm (BPS) CPE to increase robustness to non-linear phase noise without requiring additional OH. The pilot-based CPE ensured no cycle slip and provided accurate base tracking for each frame. Following this, a narrow search range BPS ($\ll \pi/2$) tracked any residual variations. Using BPS alone was not stable as the tracking was inaccurate and cycle slips frequent due to the low SNR at long transmission distances. After this, we estimated the generalized mutual information (GMI) [19] using about 10^6 bits per measured frame and averaged over 5 separate measurement batches.

4 Results

In order to maximize the SE we first optimized the rate of each channel to balance loss in SE from guard-bands and SNR degradation from linear cross-talk. This is shown in Fig. 3 for PM-64QAM and PM-256QAM. In both cases, we found that the optimal symbol rate was 21.5 GBaud, leaving about 600 MHz of guard-band corresponding to 2.7% OH. In Fig. 3 we also observe that although PM-256QAM is far away from its maximum information content of 16 bits/4D-symbol, it still gives about 0.5 bit/4D-symbol higher SE compared to PM-64QAM, at the expense of assuming significantly stronger forward error correction (FEC).
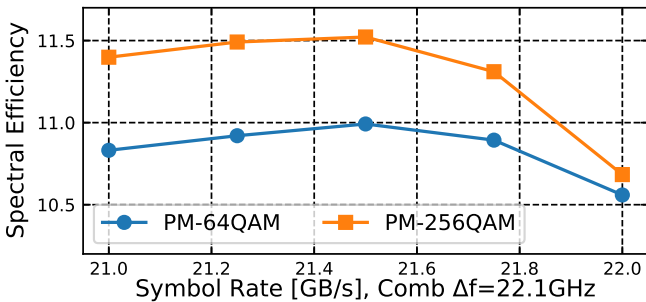

Fig. 3 Symbol rate optimization to maximize the spectral efficiency by balancing guard band overhead and cross-talk penalty.

The measured GMI after single span transmission (after deducting the pilot OH) is shown in Fig. 4a. We observe that PM-16QAM is limited by its maximum information capacity of 8 bits/4D-symbol. The average GMI was 10.3 bits/4D-symbol and 10.6 bits/4D-symbol for PM-64QAM and PM-256QAM, respectively. Deducting the guard-band OH, the SE was 10.0 and 10.3 bits/s/Hz, respectively, equivalent to a superchannel throughput of 11.5 Tb/s and 11.9 Tb/s, respectively.

The individual GMI values for all channels at distances of 164, 656, 2132 and 3116km, respectively are shown in Fig. 4b. At the distances shown in .Fig. 4b, the average GMI was 7.8, 7.3, 6.9 and 6.3 bits/4D-symbol, respectively. At the longest distance measured, 3116 km, this corresponds to 6.1 bits/s/Hz SE or equivalently a throughout of 7.0 Tb/s. Figure 4c shows the superchannel SE and throughput as a function of distance for both PM-16QAM and PM-64QAM. The insert shows constellation diagrams (X-pol) for the center channel at 1555.08 nm.

5 Conclusion

We have demonstrated a spectral efficiency of 10.4 bits/s/Hz for single span transmission and 6.1 bits/s/Hz after 3116 km for a 52 channel superchannel formed using an optimized soliton micro-comb. Exploiting the narrow line spacing and flat envelope of the optimized 22.1 GHz-spaced comb source, record spectral efficiency using a chip-scale comb device is demonstrated for all considered distances and configurations. Furthermore, the demonstrated spectral efficiency is directly comparable to systems using equivalent rates but bulk-optic frequency combs, showing that micro-combs can enable integrated superchannel transceivers on a micro-scale.

6 Acknowledgements

7 References

[1] P. J. Winzer, D. T. Neilson, and A. R. Chraplyvy, "Fiber-optic transmission and networking: the previous 20 and the next 20 years [invited]," *Optics Express*, vol. 26, no. 18, pp. 24 190–24 239, 2018.

[2] J. Rahn, L. Dardis, D. Krause, M. Rice, C. Berry, A. Kumpera, A. Nilsson, X. Xu, K. Croussore, P. Samra, K. Weidner, Z. Morbi, S. DeMars, A. Vasilyev, C. Chen, and P. Freeman, "DSP-enabled frequency locking for near-nyquist spectral efficiency superchannels utilizing integrated photonics," in *Proceedings of Optical Fiber Communication Conference*, 2018, paper W1B.3.

[3] E. Yamada, H. Takara, T. Ohara, K. Sato, T. Morioka, K. Jinguji, M. Itoh, and M. Ishii, "A high SNR, 150 ch supercontinuum CW optical source with precise 25 GHz spacing for 10 Gbit/s DWDM systems," in *Proceedings of Optical Fiber Communication Conference*, 2001, paper ME2-1.

[4] T. Ohara, H. Takara, T. Yamamoto, H. Masuda, T. Morioka, M. Abe, and H. Takahashi, "Over-1000-channel ultradense WDM transmission with supercontinuum multicarrier source," *Journal of Lightwave Technology*, vol. 24, no. 6, pp. 2311–2317, 2006.

[5] S. L. Olsson, J. Cho, S. Chandrasekhar, X. Chen, E. C. Burrows, and P. J. Winzer, "Record-high 17.3-bit/s/Hz spectral efficiency transmission over 50 km using probabilistically shaped PDM 4096-QAM," in *Proceedings of Optical Fiber Communication Conference*, 2018, paper. Th4C.5.

[6] P. Marin-Palomo, J. N. Kemal, M. Karpov, A. Kordts, J. Pfeifle, M. H. Pfeiffer, P. Trocha, S. Wolf, V. Brasch, M. H. Anderson, R. Rosenberger, V. Kovendhan, W. Freude, T. J. Kippenberg, and C. Koos, "Microresonator-based solitons for massively parallel coherent optical communications," *Nature*, vol. 546, no. 7657, pp. 274–279, 2017.

[7] B. Stern, X. Ji, Y. Okawachi, A. L. Gaeta, and M. Lipson, "Battery-operated integrated frequency comb generator," *Nature*, vol. 562, pp. 401–405, 2018.

[8] D. T. Spencer, T. Drake, T. C. Briles, J. Stone, L. C. Sinclair, C. Fredrick, Q. Li, D. Westly, B. R. Ilic, A. Bluestone, N. Volet, T. Komljenovic, L. Chang, S. H. Lee, D. Y. Oh, M.-G. Suh, K. Y. Yang, M. H. P. Pfeiffer, T. J. Kippenberg, E. Norberg, L. Theogarajan, K. Vahala, N. R. Newbury, K. Srinivasan, J. E. Bowers, S. A. Diddams, and S. B. Papp, "An optical-frequency synthesizer using integrated photonics," *Nature*, vol. 557, no. 7703, pp. 81–85, 2018.

[9] Z. L. Newman, V. Maurice, T. E. Drake, J. R. Stone, T. C. Briles, D. T. Spencer, C. Fredrick, Q. Li, D. Westly, B. R. Ilic, B. Shen, M. G. Suh, K. Y. Yang, C. Johnson, D. M. S. Johnson, L. Hollberg, K. Vahala, K. Srinivasan, S. A. Diddams, J. Kitching, S. B. Papp, and M. T. Hummon, "Photonic integration of an optical atomic clock." preprint at arXiv.

[10] J. Pfeifle, V. Brasch, M. Lauermann, Y. Yu, D. Wegner, T. Herr, K. Hartinger, P. Schindler, J. Li, D. Hillerkuss, R. Schmogrow, C. Weimann, R. Holzwarth, W. Freude, J. Leuthold, T. J. Kippenberg, and C. Koos, "Coherent terabit communications with microresonator Kerr frequency combs," *Nature Photonics*, vol. 8, no. 5, pp. 375–380, 2014.

[11] J. Pfeifle, A. Coillet, R. Henriet, K. Saleh, P. Schindler, C. Weimann, W. Freude, I. V. Balakireva, L. Larger, C. Koos, and Y. K. Chembo, "Optimally coherent kerr combs generated with crystalline whispering gallery mode resonators for ultrahigh capacity fiber communications," *Physical Review Letters*, vol. 114, no. 9, 2015.

[12] A. Fülöp, M. Mazur, A. Lorences-Riesgo, T. A. Eriksson, P.-H. Wang, Y. Xuan, D. E. Leaird, M. Qi, P. A. Andrekson, A. M. Weiner, and V. Torres-Company, "Long-haul coherent communications using microresonator-based frequency combs," *Optics Express*, vol. 25, no. 22, pp. 26 678–26 688, 2017.

[13] A. Fülöp, M. Mazur, A. Lorences-Riesgo, Ó. B. Helgason, P.-H. Wang, Y. Xuan, D. E. Leaird, M. Qi, P. A. Andrekson, A. M. Weiner, and V. Torres-Company, "High-order coherent communications using mode-locked dark-pulse Kerr combs from microresonators," *Nature Communications*, vol. 9, p. 1598, 2018.

[14] M. Mazur, J. Schroder, A. Lorences-Riesgo, M. Karlsson, and P. A. Andrekson, "Optimization of low-complexity pilot-based DSP for high spectral efficiency 51×24 Gbaud PM-64QAM transmission," in *Proceedings of European Conference on Optical Communication*, 2018, paper MoF4.2.

[15] H. Lee, T. Chen, J. Li, K. Y. Yang, S. Jeon, O. Painter, and K. J. Vahala, "Chemically etched ultrahigh-Q wedge-resonator on a silicon chip," *Nature Photonics*, vol. 6, no. 6, pp. 369–373, 2012.

[16] M.-G. Suh and K. J. Vahala, "Soliton microcomb range measurement," *Science*, vol. 359, no. 6378, pp. 884–887, 2018.

[17] X. Yi, Q.-F. Yang, K. Y. Yang, and K. Vahala, "Theory and measurement of the soliton self-frequency shift and efficiency in optical microcavities," *Optics Letters*, vol. 41, no. 15, pp. 3419–3422, 2016.

[18] J. Schroeder and M. Mazur, "Chalmersphotonicslab/qampy: V0.1," 2018, https://github.com/ChalmersPhotonicsLab/QAMpy.

[19] A. Alvarado, E. Agrell, D. Lavery, R. Maher, and P. Bayvel, "Replacing the soft-decision FEC limit paradigm in the design of optical communication systems," *Journal of Lightwave Technology*, vol. 34, no. 2, pp. 707–721, 2016.